



## On the Dynamic Behaviour of Glass Fiber-Reinforced Plastic Pipe with Clamp-Clamp Boundary Condition

Obuh Raphael Empire<sup>a</sup> Osamudiamen Efosa<sup>b\*</sup>, Edelugo Sylvester Onyemaechi<sup>c</sup>

<sup>a</sup>, <sup>c</sup>Department of Mechanical Engineering, University of Nigeria, Nsukka, Enugu State

<sup>b</sup> Department of Mechanical Engineering, University of Benin, Benin City, Nigeria

\*Email: [o.efosa@uniben.edu](mailto:o.efosa@uniben.edu)

### ARTICLE INFORMATION

#### Article history:

Received 27 February 2019

Revised 10 March 2019

Accepted 22 March 2019

Available online 29 March 2019

#### Keywords:

Dynamic analysis, GRP, FEA,  
Modal Analysis

### ABSTRACT

*A comparative analysis of the responses of glass fiber-reinforced plastic pipe and ductile iron pipe under dynamic excitation is presented in this article. The aim of the investigation was to gain insights for possible replacement of DI pipes with GRP pipes for some stringent applications. The ANSYS FEA R19.0 was used to develop the finite element model which used PIPE289 3-D 3-node element to achieve discretization of the solution domain, to which a clamp-clamp boundary condition was applied. The numerical simulation was performed on a duo-core, 8G RAM computer with convergence achieved after 4mins of simulation time. Simulation results of modal and harmonic analysis was validated against results obtained from ref [23]. Six lateral vibration modes were identified as significant for both pipes. The comparative analysis of the performance of the different pipes showed that for same mode shape numbers, GRP pipes experienced higher lateral deformation values and higher modal frequencies. Harmonic frequency and von Mises stress were higher for GRP pipe than DI pipe. A significant insight is that the stress ratio for GRP pipe is only higher than DI pipe for the first four modes. This suggests that GRP pipes of equivalent bursting strength as the DI pipe will perform better at applications prone to higher excitation frequencies.*

## 1. Introduction

Glass fiber-reinforced plastic (GRP) pipes are becoming very attractive for industrial and domestic applications due to their combined light-weight and strength characteristics, as well as excellent corrosion resistance properties [1-4]. They are suitable for water, oil and gas transportation and are cheaper compared to ductile iron (DI) pipes [5]. These desirable characteristics continue to be the basis for pushing the boundaries of application of GRP pipes thus necessitating further investigation for insights about their performance in various application environments. For example, considerations have been given to the deployment of GRP pipes as flexible subsea pipelines and risers. The response of GRP to static external and internal pressure loading under hydrostatic conditions and creep have been severally investigated [6-11]. The response of GRP to fluid structure interaction (FSI) is also very important. Generally, the dynamic stability of pipes is one such investigation that provides insight into the behavior of pipes under fluid loading under dynamic conditions. Though considerable research has been done on dynamic stability of pipes [12-18], pipes manufactured of GRP materials have not been adequately researched. The focus of dynamic stability study is the buckling and vibration of initially static pipes under the influence of fluid excitation [17,18].

Different methods have been employed to model dynamic stability phenomena of pipes conveying fluids. These methods include (i) theoretical models [19-23], (ii) finite element models [24-28], and (iii) isogeometric models [29-31]. These methods are validated with experimental results which are expensive to conduct. A generally accepted method to reduce experimentation cost and time in studies relating to dynamic analysis is by numerical methods such as FE methods which are validated using analytical results. Further argument for numerical methods is that experiments are expensive to conduct, consume more time, and cannot be used in all stages of the design process. In this study, a finite element model was developed using ANSYS R19.0 software package. The model boundary condition was set to clamp-clamp to enable the investigation of upheaval and lateral buckling during the pipe's free vibration. Modal and harmonic analysis were carried out to identify the fundamental frequencies and mode shapes of the pipe. The investigation was conducted for both GRP and DI pipes. The intention is to compare the performance of GRP with DI in order to consider possible replacement of DI in more stringent applications.

## 2. Methodology

### 2.1 Finite Element Modeling

#### 2.1.1 Geometric Modeling

The ANSYS FEA software package has three different element types that can be used to model a pipe geometry with varying degrees of accuracy namely (i) BEAM189 (ii) PIPE288 (iii) PIPE289. The PIPE289 element was used to model the pipe geometry in this study because of its advantages over the BEAM189 and PIPE288. PIPE289 is a quadratic three-node pipe element in 3-Dimension based on Timoshenko beam theory which accounts for shear-deformation effects and stress stiffness terms. This makes the elements suitable for analyzing flexural, lateral and torsional stability problems [19]. Figure 1 shows the finite element model of the pipe geometry as modeled in ANSYS R19.0.

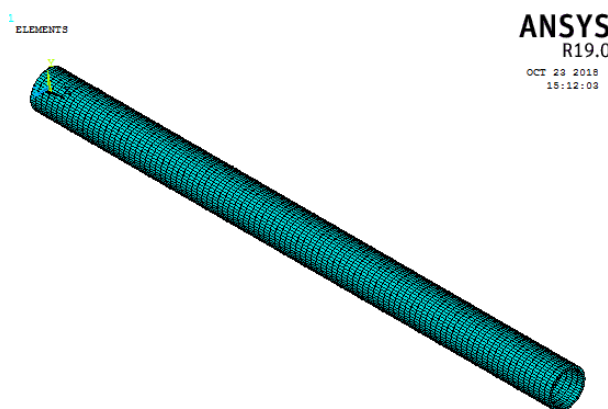


Figure 1: Finite Element Model of Pipe Geometry using ANSYS PIPE289 Elements

#### 2.1.2 Model Parameters

The parameters used in the modeling are: pipe inner diameter  $d$ , pipe thickness  $t$ , Young's modulus of elasticity of pipe material  $E$  (assumed directionally invariant for the GRP material),

and density of pipe material  $\rho$ . Table 1 presents model parameters and properties of materials used.

Table 1: Property and Parameter Table for Model

Property/Parameter	Values	
	GRP Pipe	Ductile Iron Pipe
Inner Diameter, d	254 mm	254 mm
Thickness, t	11.28 mm	6.35 mm
Density	1820 kg/m <sup>3</sup>	7086.56 kg/m <sup>3</sup>
Modulus of Elasticity	170 GN/m <sup>2</sup>	200 GN/m <sup>2</sup>

## 2.2 Model Validation

The results of the ANSYS simulation was validated against the analytical solutions obtained from Blevins' Formulas for Natural Frequencies and Mode Shapes [23]. The expressions are given as:

$$w_n = \lambda^2 \sqrt{\frac{EI}{ML^4}} \quad (1)$$

The governing differential equation is given by:

$$EI \frac{\partial^4 y}{\partial x^4} + \rho A v^2 \frac{\partial^2 y}{\partial x^2} + 2\rho A v \frac{\partial^2 y}{\partial x \partial t} + M \frac{\partial^2 y}{\partial t^2} = 0 \quad (2)$$

To solve this equation, the following boundary conditions are applied:

$$Y(0, t) = Y(L, t) = 0 \quad (3)$$

$$\frac{\partial^2 y}{\partial x^2}(0, t) = \frac{\partial^2 y}{\partial x^2}(L, t) = 0 \quad (4)$$

The eigenvalues solution of the first six modes from Equation (2) is given as:

$$\left. \begin{aligned} \lambda^2_1 &= 1.506\pi \\ \lambda^2_2 &= 2.50\pi \\ \lambda^2_3 &= 3.450\pi \\ \lambda^2_4 &= 4.501\pi \\ \lambda^2_5 &= 5.35\pi \\ \lambda^2_6 &= 6.55\pi \end{aligned} \right\} \quad (5)$$

These values are used to compute the natural frequencies from Equation (1) and the results compared with those from ANSYS as shown Figure 2.

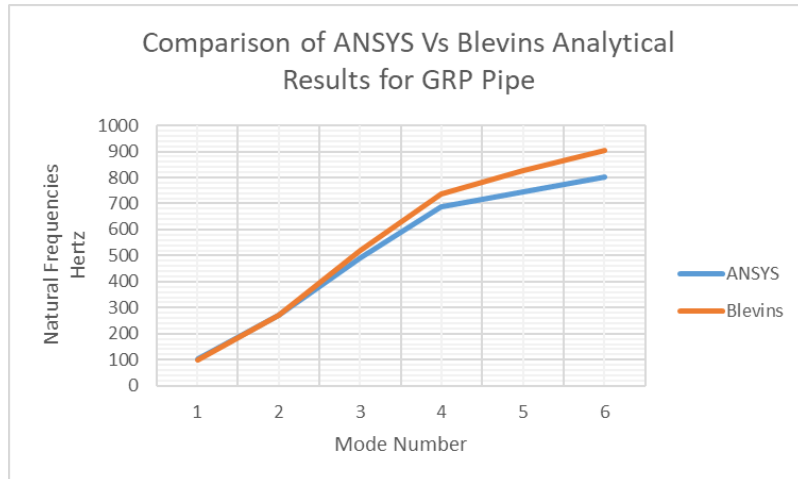


Figure 2: Model Validation of ANSYS Formulation against Blevins Analytical Solution

### 3. Results and Discussion

The contour plots of the results of the first six mode shapes and the corresponded equivalent von Mises stresses are displayed in Figures 3 to 8. Figures 3 and 4 display same mode shape (buckle) for mode 1 and 2 but different deformation orientations with Figure 3 oriented in the y-axis (upheaval buckling) and Figure 4 oriented in the x-axis (lateral buckling or snaking). Plots (A) and (B) compares the modal shape and frequencies for GRP pipe and DI pipe respectively while plots (C) and (D) are the corresponded equivalent von Mises stresses. It is observed that for both modes, GRP pipe experienced more deformation and stress and at higher modal frequency than DI pipe. Figures 5 and 6 display same mode shapes (buckle) for modes 3 and 4 but different deformation orientations with Figure 5 oriented in the y-axis (upheaval buckling) and Figure 6 oriented in the x-axis (lateral buckling or snaking). Plots (A) and (B) compares the modal shape and frequencies for GRP pipe and DI pipe respectively while plots (C) and (D) are the corresponded equivalent von Mises stresses. It is observed that for both modes, GRP pipe experienced more deformation and stress and at higher modal frequency than DI pipe. Figures 7 and 8 display same mode shape (buckle) for mode 5 and 6 but different deformation orientations with Figure 7 oriented in the y-axis (upheaval buckling) and Figure 8 oriented in the x-axis (lateral buckling or snaking). Plots (A) and (B) compares the modal shape and frequencies for GRP pipe and DI pipe respectively while plots (C) and (D) are the corresponded equivalent von Mises stresses. It is observed that for both modes, GRP pipe experienced more deformation and stress and at higher modal frequency than DI pipe.

Figure 9 is a graphical plot of mode shape numbers against modal frequencies for GRP and DI pipes. From the plot, it is evident that GRP pipe conforms to the different mode shapes at higher frequencies compared to DI, and the frequency values are more divergent with increasing mode number.

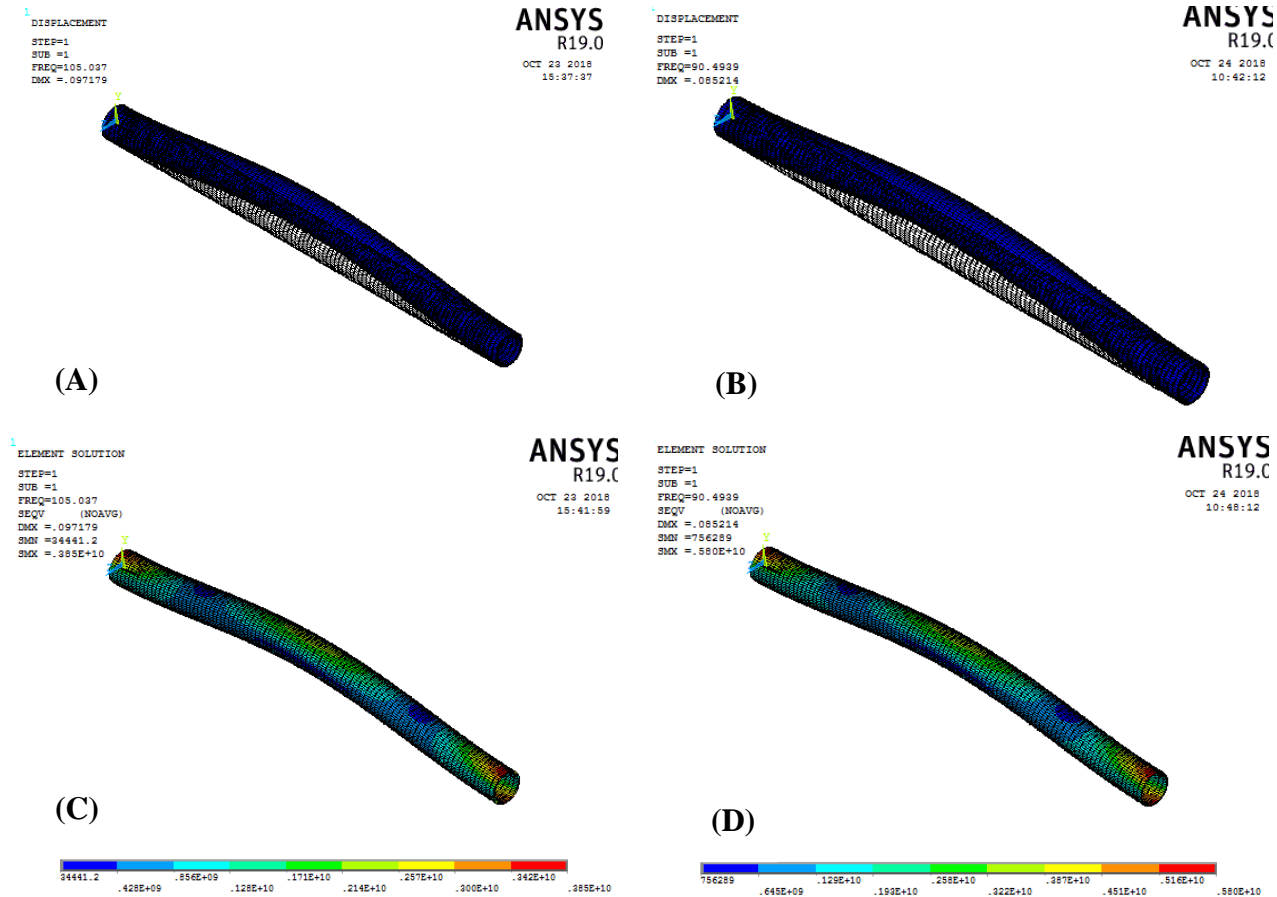


Figure 3: Modal Shape and Stress for Mode 1 - (A) & (C) GRP, (B) & (D) DI

Figure 10 shows that lateral deformation of both GRP and DI pipes remain fairly constant with GRP pipe having higher values per mode shape for the first six mode shapes. The outliers are values for the bursting modes which is mode 7 for GRP pipe and mode 10 for DI pipe. The equivalent von Mises stresses increases with increasing mode number for both GRP and DI, with GRP having higher stress values. This observation with respect to equiv. von Mises stresses may not be too informative to aid decision on deployment of GRP. The concept of stress ratio (*ratio equiv. von Mises stress to material yield stress*) was adopted as a more informative index for comparing the performance of the pipes with respect to equiv. von Mises stresses. Figure 12 shows that DI pipes have lower stress ratios than GRP pipes for the first four modes, and then becomes higher at higher mode numbers. It thus be inferred that GRP pipes of equivalent bursting strength as DI can replace DI at stringent applications subject to high excitation frequencies. Figures 13 and 14 are results of the harmonic frequency analysis again showing that GRP pipes exhibit conformity at higher frequencies than DI pipes. These results are insightful and thus open experimental investigation efforts to further validate the possibility of deploying GRP pipes for more stringent applications instead of DI.

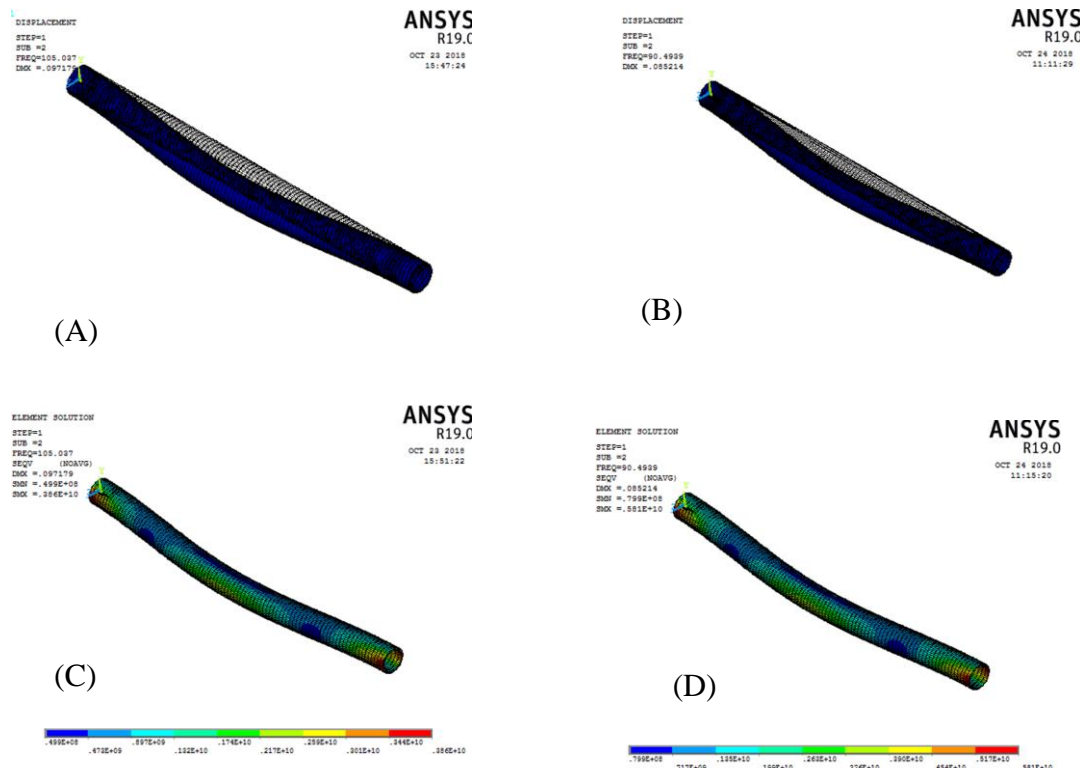


Figure 4: Modal Shape and Stress for Mode 2 - (A) & (C) GRP, (B) & (D) DI

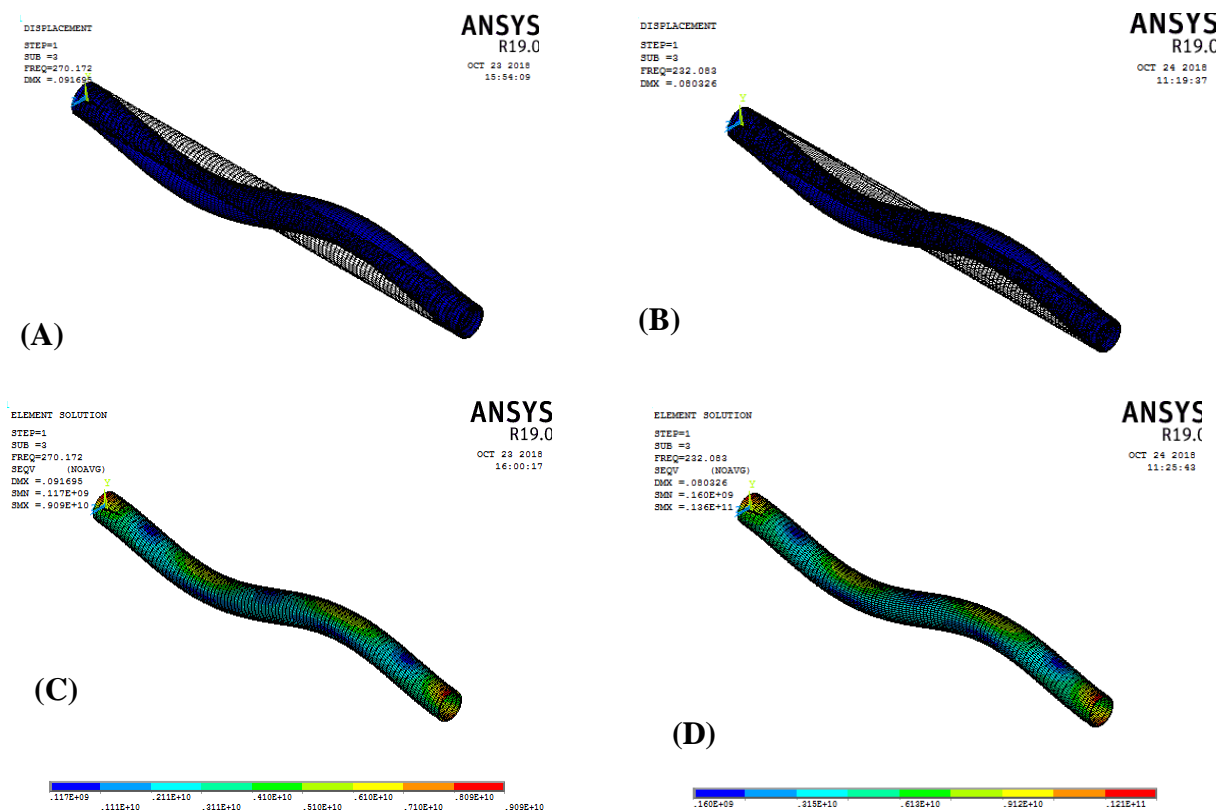


Figure 5: Modal Shape and Stress for Mode 3 - (A) & (C) GRP, (B) & (D) DI

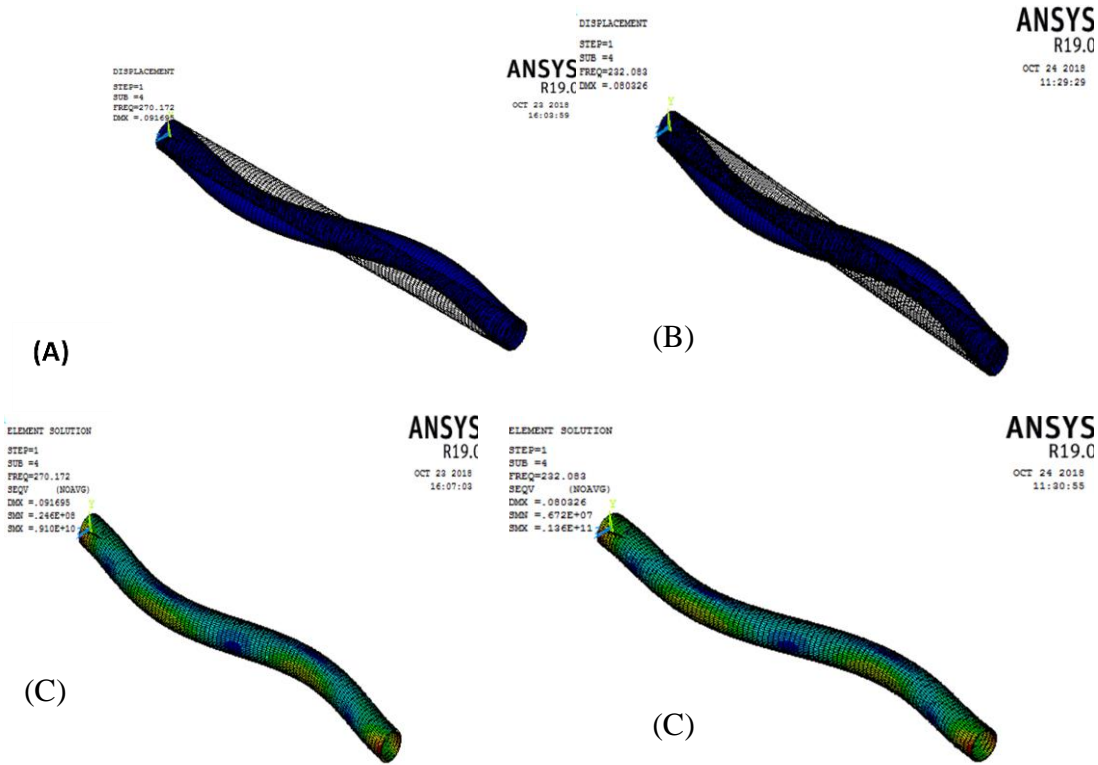


Figure 6: Modal Shape and Stress for Mode 4 - (A) & (C) GRP, (B) & (D) DI

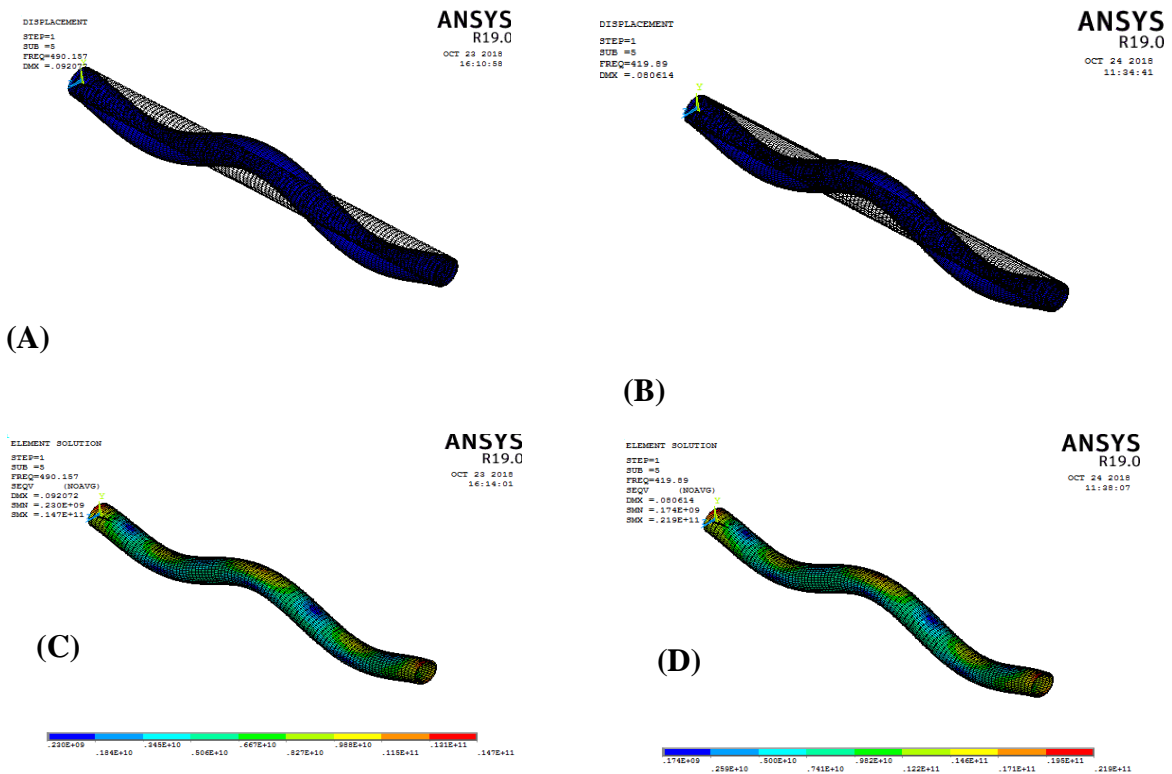


Figure 7: Modal Shape and Stress for Mode 5 - (A) & (C) GRP, (B) & (D) DI

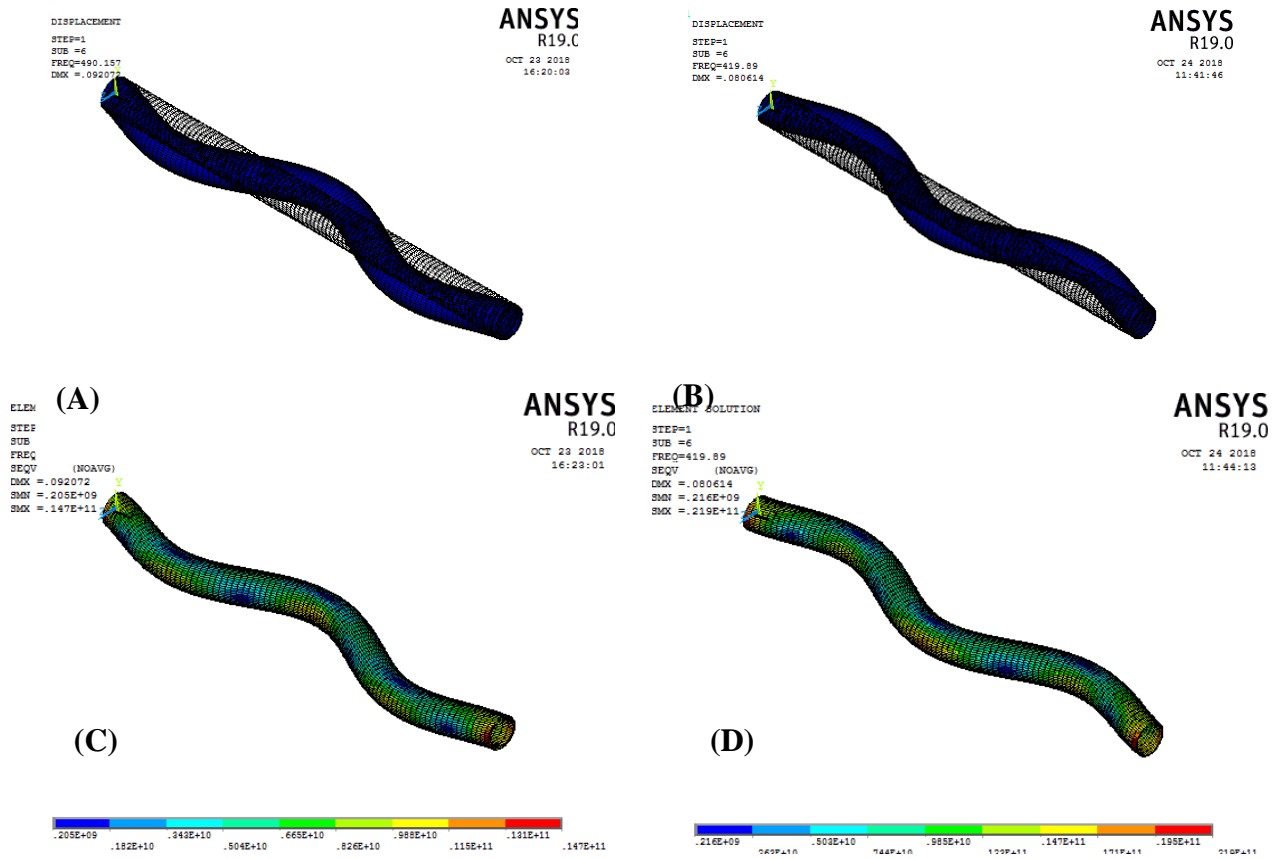


Figure 8: Modal Shape and Stress for Mode 6 - (A) & (C) GRP, (B) & (D) DI

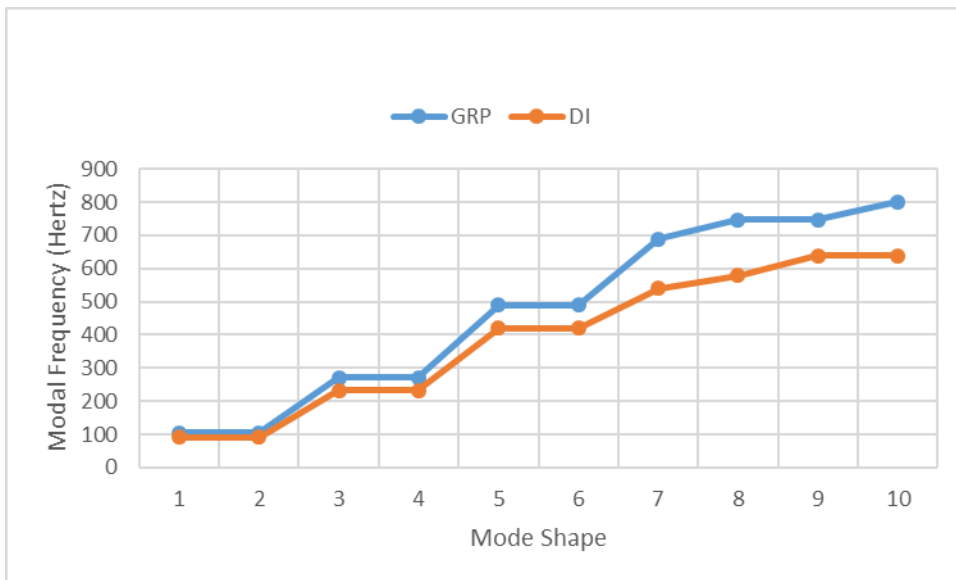


Figure 9: Graph of Mode Shape vs Modal Frequencies

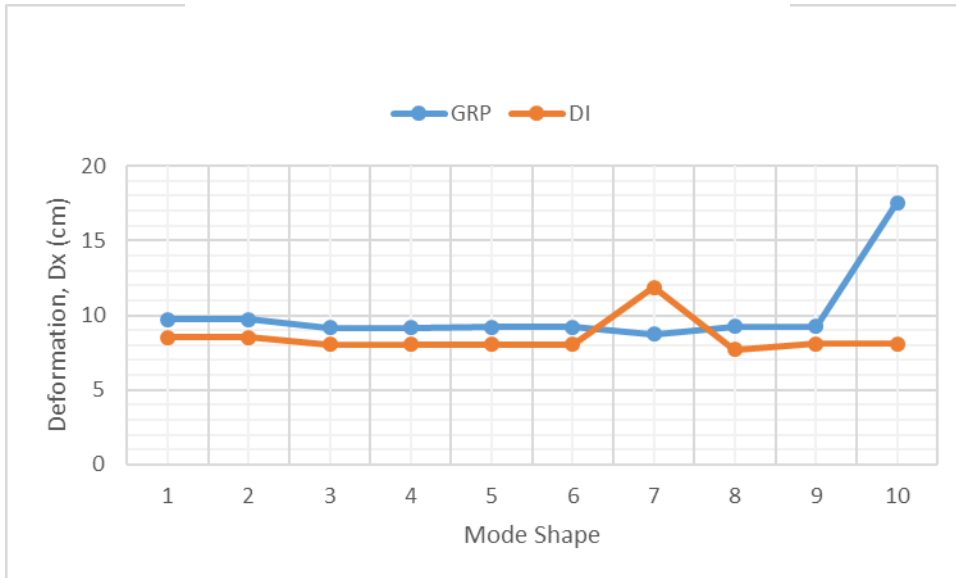


Figure 10: Mode Shape vs Lateral Deformation

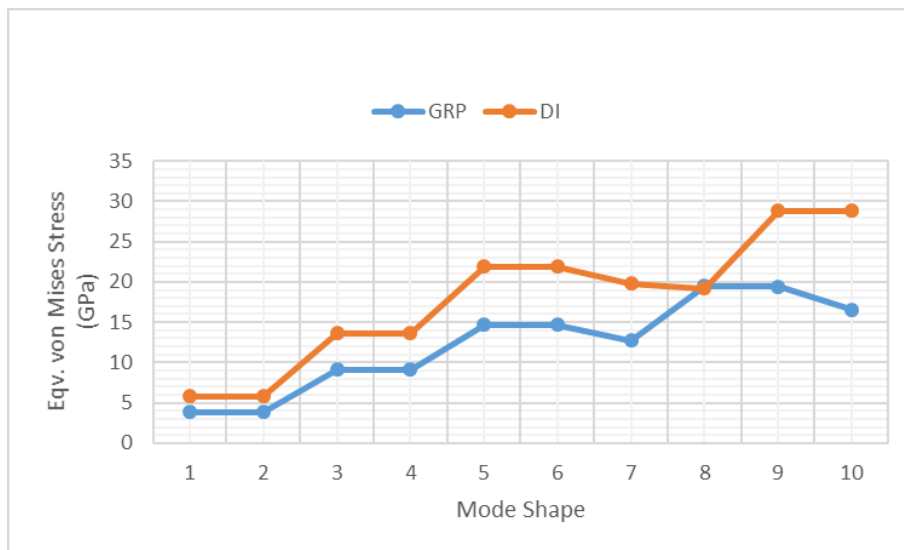


Figure 11: Mode Shape vs Equiv. von Mises Stress

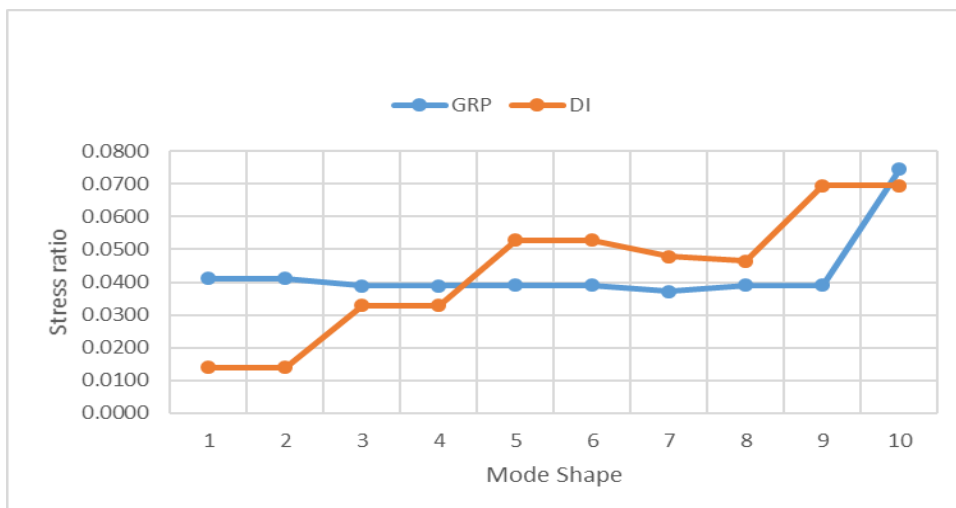


Figure 12: Mode Shape vs Stress ratio

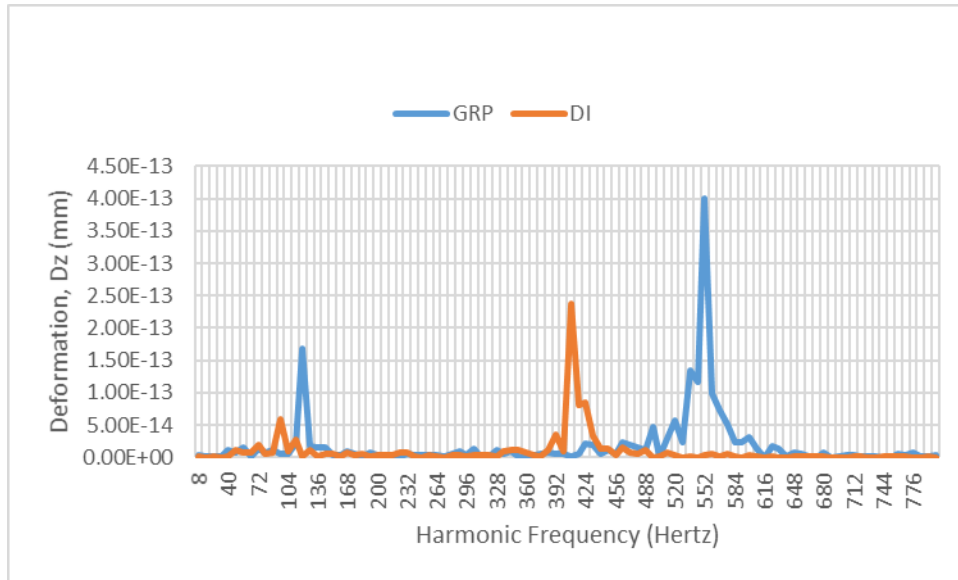


Figure 13: Harmonic Frequencies vs Axial Deformation

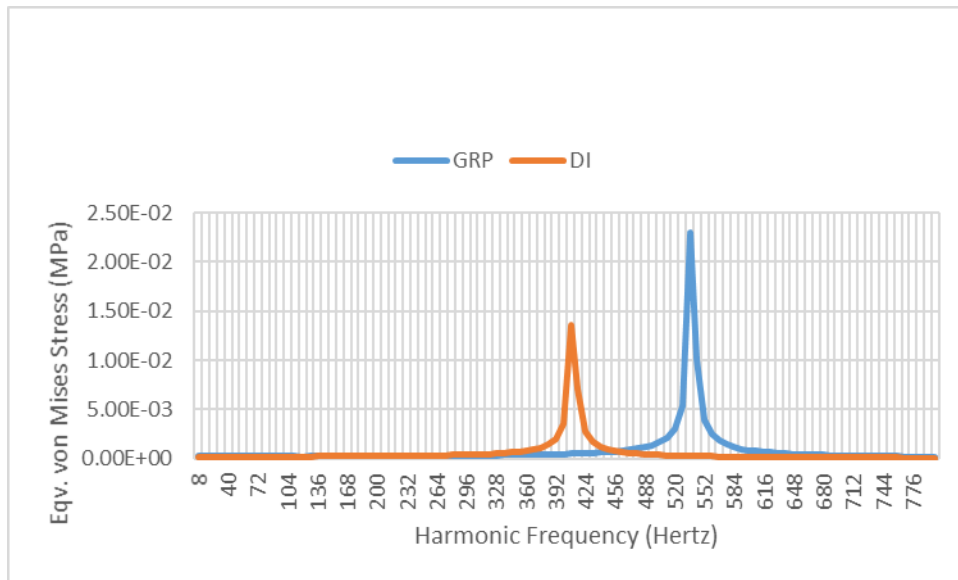


Figure 14: Harmonic Frequencies vs Equiv. von Mises Stress

#### 4. Conclusion

In this paper, a computational method was adopted to develop a finite element model of a pipe conveying water to investigate the dynamics of GRP pipe in comparison with DI pipe. The ANSYS FEA R19.0 was used to develop the finite element model which used PIPE289 3-D 3-node element to achieve discretization of the solution domain, to which a clamp-clamp boundary condition was applied. The numerical simulation was performed on a duo-core, 8G RAM computer with convergence achieved after 4mins of simulation time. Simulation results of modal and harmonic analysis was validated against results obtained from ref [23]. Six lateral vibration modes were identified as significant for both pipes. The comparative analysis of the performance of the different pipes show that for same mode shape numbers, GRP pipes experienced higher lateral

deformation values and higher modal frequencies. Harmonic frequency and von Mises stress were higher for GRP pipe than DI pipe. A significant insight is that the stress ratio for GRP pipe is only higher than DI pipe for the first four modes. This suggests that GRP pipes of equivalent bursting strength as the DI pipe will perform better at applications prone to higher excitation frequencies.

## Nomenclature

$A$	Pipe internal area ( $m^2$ )
$E$	Young's modulus for the pipe material ( $N/m^2$ )
$I$	Second moment of area of the pipe cross section ( $m^4$ )
$L$	Total length of the pipe (m)
$M$	Combined mass per unit length of the pipe material and fluid (kg)
$v$	Flow velocity (m/s)
$Y(x,t)$	Transverse deflection (m)
$\lambda$	Eigenvalue
$\rho$	Fluid density ( $kg/m^3$ )

## 5. Conflict of Interest

There is no conflict of interest associated with this work.

## References

- [1] H. El-Hassan, T. El-Maaddawy, A. Al-Sallamin, A. Al-Saidy (2018). Durability of glass fiber-reinforced polymer bars conditioned in moist seawater-contaminated concrete under sustained load, *Construction and Building Materials*, Vol. 175, pp. 1-13
- [2] M. Robert, P. Cousin, B. Benmokrane (2009). Durability of GRP reinforcing bars embedded in moist concrete, *J. Compos. Constr.* Vol. 13 (2), pp. 66–73.
- [3] Z. Wang, X.-L. Zhao, G. Xian, G. Wu, R.K. Singh Raman, S. Al-Saadi, A. Haque (2017). Long-term durability of basalt- and glass-fibre reinforced polymer (BFRP/GRP) bars in seawater and sea sand concrete environment, *Constr. Build. Mater.* Vol. 139, pp. 467–489.
- [4] A. Mukherjee, S.J. Arwihar (2005). Performance of glass fiber-reinforced polymer reinforcing bars in tropical environments – part I: structural scale tests, *Struct. J.* Vol. 102 (5), pp2-15
- [5] G. Capiel, P. Fayó, A. Orofino, P. E. Montemartini (2016). Failure of glass fiber-reinforced epoxy pipes in oil fields, *Handbook of Materials Failure Analysis With Case Studies from the Oil and Gas Industry*, Chapter 4, pp. 91-101
- [6] J.F. Davalos, Y. Chen, I. Ray (2012). Long-term durability prediction models for GRP bars in concrete environment, *J. Compos. Mater.* Vol. 46 (16) pp. 1899–1914.
- [7] Y.A. Al-Salloum, T.H. Almusallam (2007). Creep effect on the behavior of concrete beams reinforced with GRP bars subjected to different environments, *Constr. Build. Mater.* Vol. 21 (7) pp. 1510–1519.
- [8] H. Fergani, M. Guadagnini, C. Lynsdale, C. Mias, M. Di Benedetti (2016). Long term performance of GRP bars under the combined effects of sustained load and severe environments, in: 8th International Conference on Fibre-Reinforced Polymer (FRP) Composites in Civil Engineering (CICE 2016), Hong Kong, China.
- [9] H. Fergani, M. Di Benedetti, M. Guadagnini, C. Lynsdale, C. Mias (2017). Characterization and durability study of GRP bars exposed to severe environments and under sustained loads, in: 5th International Conference on Durability of Fiber Reinforced Polymer (FRP) Composites for Construction and Rehabilitation of Structures (CDCC 2017), Sherbrooke, Quebec, Canada.
- [10] H. Fergani, M. Di Benedetti, C. Miàs Oller, C. Lynsdale, M. Guadagnini (2018). Longterm performance of GRP bars in concrete elements under sustained load and environmental actions, *Compos. Struct.* Vol. 190 pp. 20–31.

- [11] K. Laoubi, E. El-Salakawy, B. Benmokrane (2006). Creep and durability of sand-coated glass FRP bars in concrete elements under freeze/thaw cycling and sustained loads, *Cem. Concr. Compos.*, Vol. 28 (10) pp. 869–878.
- [12] A. Zare, M. Eghtesad, F. Daneshmand (2017). Numerical investigation and dynamic behavior of pipes conveying fluid based on isogeometric analysis, *J. Ocean Engineering*, Vol. 140, pp. 388-400
- [13] O. J. Aldraihem (2007). Analysis of the dynamic stability of collar-stiffened pipes conveying fluid. *J. Sound Vibr.* Vol. 300 (3–5), pp. 453–465.
- [14] P. A. Hansson, G. Sandberg (2001). Dynamic finite element analysis of fluid-filled pipes. *Comput. Methods Appl. Mech. Eng.* Vol. 190 (24–25), pp. 3111–3120.
- [15] Y. Modarres-Sadeghi, M. P. Païdoussis (2009). Nonlinear dynamics of extensible fluid conveying pipes, supported at both ends. *J. Fluids Struct.* Vol. 25 (3), pp. 535–543.
- [16] T. Zhang, H. Ouyang, Y. O. Zhang, B. L. Lv (2016). Nonlinear dynamics of straight fluid-conveying pipes with general boundary conditions and additional springs and masses. *Appl. Math. Model.* Vol. 40 (17–18), pp. 7880–7900.
- [17] F. Liang, Y. Xiao-Dong, Z. Wei, Q. Ying-Jing (2018). Dynamic modeling and free vibration analysis of spinning pipes conveying fluid with axial deployment, *Journal of Sound and Vibration*, Vol. 417, pp. 65-79.
- [18] M.P. Païdoussis (2014) *Fluid-structure Interactions: Slender Structures and Axial Flow*, second ed., vol. 1, Academic Press, London.
- [19] M. P. Païdoussis, and M. T. Issid (1973). Dynamic stability of pipes conveying fluid, *Journal of Sound and Vibration*, Vol. 33(3), pp. 267-294.
- [20] D. G. Gorman, J. M. Reese, and Y. I. Zhang (2000). Vibration of flexible pipe conveying viscous pulsating fluid flow, *J. Sound Vib.*, Vol. 230(2), pp. 379-392.
- [21] U. Lee, C. H. Park, and S. C. Hong (1995). The dynamics of a piping system with internal unsteady flow, *J. Sound Vib.*, Vol. 180(2), pp. 297-311.
- [22] L. Zhang, A. S. Tijsseling, and A. E. Vardy (1995). Frequency response analysis in internal flows, *J. Hydrodynam, Series B* Vol. 3(3), pp. 39-49
- [23] R. D. Blevins (1979). *Formulas for Natural Frequency and Mode Shape*, New York: Van Nostrand Reinhold
- [24] O. C. Zienkiewicz, P. Bettess (1978). Fluid-structure dynamic interaction and wave forces: an introduction to numerical treatment, *International Journal of Numerical Methods in Engineering*, Vol. 13, pp. 1-16
- [25] A. G. T. J. Heinsbroek, C. S. W. Lavooij, A. S. Tijsseling (1991). Fluid-structure interaction in non-rigid piping – a numerical investigation, *Transaction of SMiRT11*, Tokyo, Japan, pp. 309-314.
- [26] A. G. T. J. Heinsbroek and A. S. Tijsseling (1993). Fluid-structure interaction in non-rigid piping systems – a numerical investigation II, *Transaction of SMiRT12*, Stuttgart, Germany, p. Paper J08/2.
- [27] A. G. T. J. Heinsbroek (1993). Fluid-structure interaction in non-rigid pipeline systems – comparative analyses, *ASME/TWI 12<sup>th</sup> International Conf. on Offshore Mechanics and Arctic Engineering*, Glasgow, UK, p. Paper OMAE-93-1018, 405-410.
- [28] W. Erath, B. Nowotny, and J. Maetz (1998). Simultaneous coupling of the calculation of pressure waves and pipe oscillations, *3R International*, Vol. 37, pp. 501-508.
- [29] A. Zare, M. Eghtesad, F. Daneshmand (2018). An isogeometric analysis approach to the stability of curved pipes conveying fluid, *Marine Structures*, Vol. 59, pp. 321-341.
- [30] B. S. Hosseini, M. Moller, S. Turek (2015). Isogeometric Analysis of the Navier-Stokes equations with Taylor-Hood B-spline elements, *Applied Mathematics and Computation*, Vol. 267, pp. 264-281.
- [31] L. Engvall, J. A. Evans (2017). Isogeometric unstructured tetrahedral and mixed-element Bernstein-Bezier discretization, *Computer Methods in Applied Mechanics and Engineering*, Vol. 319, pp. 83-123